Article:
Hu, Q., Zhang, L., Luo, Q. et al. (5 more authors) (2024) Impact of polycarboxylate superplasticizer dosage on controlled low strength material flowability and bleeding: Insights from water film thickness. Construction and Building Materials, 447. 138145. ISSN: 0950-0618

https://doi.org/10.1016/j.conbuildmat.2024.138145

Impact of Polycarboxylate Superplasticizer Dosage on the Flowability and Bleeding of Controlled Low Strength Material: Insights from Water Film Thickness

Qiuhui Hu [1]; **Liang Zhang** [1,2]; **Qiang Luo** [1,2]; **Ke Yu** [1]; **David P. Connolly** [3]; **Libing Qin** [1]; **Liyang Wang**[4]; **Tengfei Wang** [1,2]*

1. School of Civil Engineering, Southwest Jiaotong Univ., Chengdu 610031, China

2. Key Laboratory of High-speed Railway Engineering (Southwest Jiaotong University), Ministry of Education, Chengdu 610031, China

3. School of Civil Engineering, University of Leeds, Leeds LS2 9JT, UK

4. Railway Engineering Research Institute, China Academy of Railway Sciences Co., Ltd., Beijing 100081, China

*Corresponding author: w@swjtu.edu.cn (T. Wang); ORCID: 0000-0003-4079-0687

Abstract

Civil excavation projects frequently yield substantial excess spoil, posing challenges to sustainable construction. This study explores repurposing such spoil for creating controlled low strength material (CLSM), emphasizing the novel use of polycarboxylate superplasticizer (PCE) to reduce the water requirement. The also work distinctively utilizes water film thickness (WFT) theory to elucidate the effects of PCE dosage and WFT on material properties, thereby advancing CLSM mix design. First, using an experimental approach, a series of fresh CLSM samples are prepared, with varying the water-to-solid ratio (W/S) and PCE dosage, to evaluate their packing density, WFT, flowability, and bleeding rate. It is demonstrated that both packing density and WFT experienced a non-linear increase with rising PCE dosage. Regression analysis of the experimental data reveals that the flowability and bleeding rate linearly increase with the rising WFT, and the enhancements are more pronounced at higher PCE dosage. Notably, at a given WFT, the impact of PCE dosage on flowability and bleeding rate reduce as WFT decreases. Additionally, the research identifies specific WFT thresholds correlating with maximum flowability and a 5% bleeding rate. These thresholds mark the critical point at which WFT ceases to influence flowability and delineate the maximum WFT that satisfies the bleeding rate requirements, respectively. These insights are important for optimizing the design of CLSM with PCE in terms of flowability and bleeding rate.

Keywords: controlled low strength material; water film thickness; polycarboxylate; flowability; bleeding rate; construction spoil

1 Introduction

Underground infrastructure projects, including foundation pit excavation, subway construction, and the development of underground pipeline facilities, generate significant amounts of construction spoil [1–3]. Traditional approaches for managing this spoil predominantly involve using muck trucks to transport it to suburban landfills for what is known as stacking treatment. However, this method has several drawbacks. It not only exacerbates dust pollution and increases construction costs but also demands considerable land resources for the creation and maintenance of suburban landfills. Moreover, the disposal of construction spoil in landfills leads to environmental issues, such as land subsidence, vegetation degradation, and a heightened risk of landslides [4–6]. In light of these challenges, identifying alternative uses for construction spoil is becoming increasingly important. Repurposing this material could significantly reduce disposal costs, curtail the consumption of raw materials, and lower environmental pollution, thereby contributing to greater sustainability in construction practices [7]. Another critical issue in urban infrastructure projects is the limited operational space available for activities like road widening, pipe network installation, and abutment construction. This often affects the compaction quality of traditional backfill materials, leading to engineering problems such as uneven settlement [8,9]. Consequently, the development of a novel, self-compacting backfill material prepared from construction spoil offers promising advantages, addressing both environmental concerns and engineering challenges.

Controlled low-strength material (CLSM) is a self-compacting, cementitious material, typically used as an alternative to compacted fill and its compressive strength is below 8.3 MPa [10]. Standard CLSM mixes usually comprise water, Portland cement, fly ash or similar products, and fine or coarse

aggregates, or a combination of both. Recently, due to the scarcity of aggregate resources and challenges in spoil disposal, soil has been employed as a substitute for aggregate in CLSM preparation [11,12]. This soil-incorporated CLSM has been defined using a variety of terms such as soil–cement slurry [13], ready-mixed soil material [14], high-fluid backfill materials (HFBMs) [15], or soil-based CLSM [16]. Extensive research has been conducted on the preparation and properties of soil-based CLSM. Qian et al. [17] observed that excessive soil content can degrade performance, but if properly mixed, excess excavated soil can be effectively used in CLSM. Puppala et al. [18] designed several CLSMs using native clayey soils, demonstrating that mixes with high-plasticity clays could meet both flowability and density criteria. Additionally, Wang et al. [19] investigated the feasibility of using silty soil as the sole aggregate in CLSM, combined with local red mud (RM) and Portland cement as binders. They found RM significantly influences the engineering properties of CLSM, with an optimum RM to cement mass ratio of 0.5.

However, the small particle size and high specific surface area of construction spoils mean that CLSM prepared from such materials requires more mixing water to achieve the necessary flowability, which, in turn, diminishes the hardened strength of the CLSM. Polycarboxylate superplasticizer (PCE), a commonly used water-reducing agent known for its strong water-reducing and strength-enhancing effects, is widely employed in the concrete industry. To address the balance between flowability and strength in soil-based CLSM, several studies have investigated the use of PCE. Wan et al. [20] prepared CLSM using excavated waste soils and PCE to enhance workability. Their results showed a significant improvement in flowability with the addition of 1.0% PCE. Zhang et al. [21] used waste marine dredged clay to prepare CLSM, finding that PCE disperses both waste marine dredged clay and cement

in soil-based CLSM, improving flowability through electrostatic forces and steric hindrance. An increase in flowability was noted with 0.4% PCE content. Most current research has focused on the effect of PCE dosage on the soil-based CLSM flowability under the condition the mixing water is constant. Yet, the combined effect of the water-to-solid ratio (W/S) and PCE dosage on the improvement of flowability in soil-based CLSM remains underexplored.

Water Film Thickness (WFT) has been extensively studied as a crucial factor influencing the flowability of cement paste, mortar, and concrete [22–24]. Zhang et al. [25] theorized that the mixing water in cementitious materials could be categorized into filling water, which occupies voids between particles, and excess water, which forms a water film over particle surfaces to enhance flowability. To explore the combined effects of excess water, packing density, and solid surface area on flowability, Kwan et al. [26,27] developed a wet packing method for determining the packing density of cementitious materials, with WFT calculated as the ratio of excess water to solid surface area. Their research established WFT as the predominant factor governing the flowability of cement paste and cement–sand mortar [28,29].

Several studies also have focused on integrating superplasticizers (SP) to enhance the flowability of granular materials and exploring the combined effects of WFT and SP on flowability. Kwan et al. [30] examined the combined roles of WFT and SP dosage in mortar flow spread, finding that packing density, WFT, and flow spread all increase with SP dosage. Guo et al. [31] investigated the flowability of ultrafine-tailings cemented paste backfill (UTCPB) with SP, using WFT theory. Their findings suggested that the flow spread of fresh UTCPB could be characterized by a unary exponential-type function of WFT. Similarly, Wu et al. [32] applied WFT theory to analyze how water content and PCE

dosages affect the flow spread of phosphorus building gypsum (PBG), revealing a positive linear correlation between flow spread and WFT, though the impact of WFT diminishes with increasing PCE dosage.

Like mortar, UTCPB, and PBG, CLSM prepared from construction spoil also contains substantial granular material. However, the role of WFT in soil-based CLSM has yet to be established or applied. Therefore, this study introduces WFT theory to analyze the performances of CLSM prepared from construction spoil, specifically examining the effects of W/S and PCE dosages on the packing density, WFT, flowability, and bleeding rate of fresh CLSMs. Additionally, this research also aims to achieve higher flowability at a lower W/S by incorporating PCE, thus resolving the existing conflict between flowability and compressive strength in soil-based CLSM. To this end, a series of fresh CLSM samples were prepared with varying W/S and PCE dosages, and the combined effects of PCE dosages and WFT on the flowability and bleeding rate of soil-based CLSMs are analysed, enabling the calculation of these properties during CLSM usage.

2 Materials and methods

This section outlines the materials and methodologies employed to analyze the properties of soil-based CLSMs using various dosages of PCE. It details materials characteristics, mix proportions, and specific test methods for assessing parameters such as packing density, WFT, flowability, and bleeding rate.

2.1 Materials

In this study, soil-based Controlled Low Strength Material (CLSM) was formulated using waste red-bed mudstone, cement, PCE, and water. The waste red-bed mudstone, sourced from a construction

site in Southwestern China, underwent crushing and sieving through a 4.75 mm (No.4 sieve) to ensure its classification as fine aggregate, effectively eliminating the influence of larger gravel on subsequent laboratory tests [33]. It's physical properties were characterized according to the *Standard for Geotechnical Testing Method* (GB 50123-2019), with the key findings presented in Table 1. Notably, the soil comprises 78.9% particles smaller than 0.075 mm (No.200 sieve), and is classified by the *Unified Soil Classification System* (ASTM-D2487-17) as a low-plasticity clay (CL).

Additionally, the soil's mineral composition was determined using X-ray diffraction (XRD) analysis, performed on an X-ray diffractometer employing Cu Kα radiation at 40 kV/40 mA. The XRD results, illustrated in Fig. 1, reveal that the soil primarily consists of Quartz, Calcite, Muscovite, and Clinochlore.

Table 1. Index properties of the red-bed mudstone samples

Parameters	Values
Maximum dry density (kg/m^3)	1950
Optimum Moisture Content, OMC (%)	10.65
Natural water content (%)	4.87
Specific gravity	2.70
Liquid Limit, LL (%)	31.5
Plasticity Index, PI	17.1
Particles < 75 μm (%)	78.9
Appearance	Maroon coloured

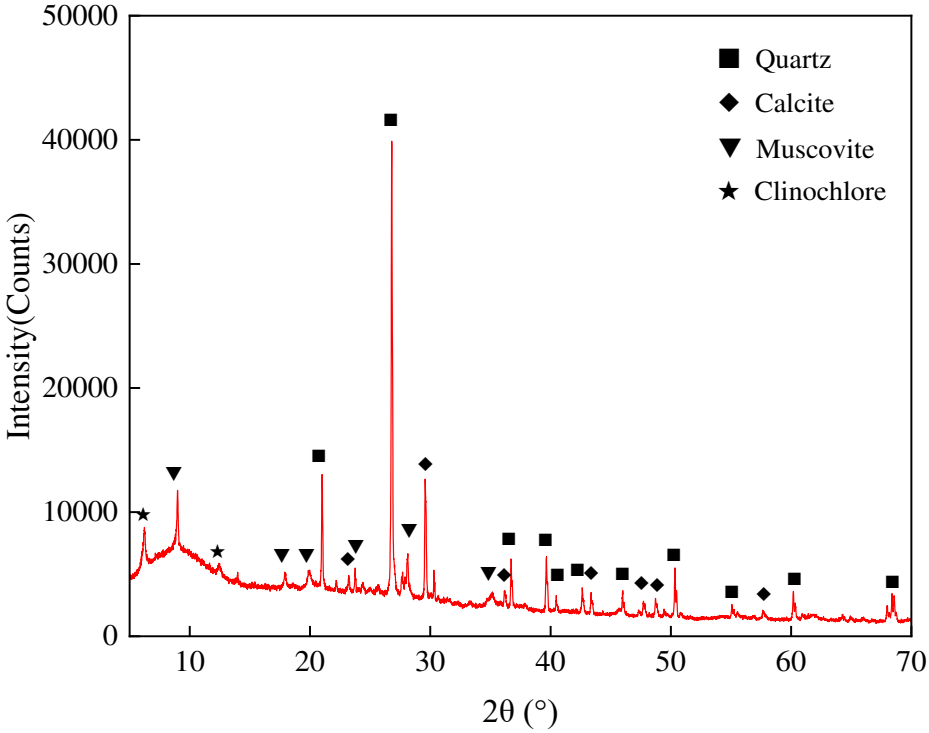

Figure 1. X-ray diffraction spectra of the red-bed mudstone

In this research, ordinary Portland cement (OPC) with a strength grade of 42.5 was utilized, adhering to the Chinese standard GB175-2007. The solid densities of the red-bed mudstone and OPC were measured as 2700 kg/m^3 and 3100 kg/m^3, respectively. Particle size distribution and average particle size of these materials were analyzed using a Malvern Mastersizer 2000 laser particle size distribution analyzer, as depicted in Fig. 2. This instrument also automatically calculated the specific surface areas based on the particle sizes. The median diameters (D_{50}) of the red-bed mudstone and OPC were 16.02 μm and 13.04 μm, respectively, with their specific surface areas determined to be 294 m^2/kg and 366 m^2/kg.

The polycarboxylate superplasticizer used in this study, designated as ZK-1, was supplied by Jizhou Yasidun Building Materials Technology Co., Ltd. (China). It is characterized by a water reduction rate of 29%. Standard tap water was employed for all experimental procedures.

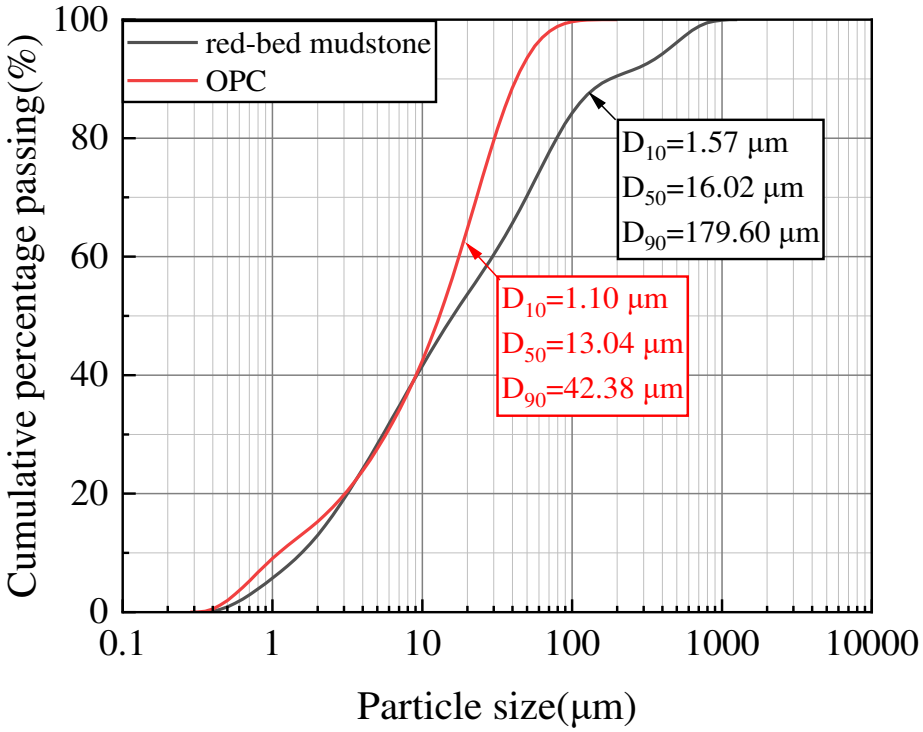

Figure 2. Particle size distributions of red-bed mudstone and OPC

2.2 Mix proportions

Regarding the examination of the impact of PCE dosage on soil-based CLSM properties, five PCE dosages were tested: 0%, 0.1%, 0.2%, 0.3%, and 0.4% of the solid particles' mass. The water-to-solid ratio (W/S), also measured by mass, were varied for different tests. Specifically, for packing density tests, the W/S ratio ranged from 24% to 40% in increments of 2%; for water film thickness (WFT) and flowability tests, the W/S ratio ranged from 32% to 58% in increments of 2%; for bleeding rate tests, the W/S ratio ranged from 34% to 54% in increments of 2%. The cement dosage for all mixes was maintained at 100 kg/m^3. This experimental setup was essential to assess the influence of different PCE dosages and W/S on the properties of the CLSM. The mix proportions for soil-based CLSM adopted in this study were detailed in Table 2.

Table 2. Mix proportions for soil-based CLSM mixes

ID	W/S (%)	Water (kg/m^3)	Cement (kg/m^3)	Dry red-bed mudstone (kg/m^3)
1	24	395.1	100	1546.2
2	26	414.4	100	1494
3	28	432.6	100	1444.9
4	30	449.7	100	1398.8
5	32	465.7	100	1355.4
6	34	480.9	100	1314.4
7	36	495.3	100	1275.7
8	38	508.8	100	1239.0
9	40	521.7	100	1204.3
10	42	533.9	100	1171.3
11	44	545.6	100	1139.9
12	46	555.6	100	1110
13	48	567.2	100	1081.6
14	50	577.2	100	1054.4
15	52	586.8	100	1028.5
16	54	596	100	1003.7
17	56	604.8	100	980
18	58	613.2	100	957.2

2.3 Sample preparation and testing methods

2.3.1 Sample preparation

Before commencing the mixing process, the water content of the red-bed mudstone was measured to determine the mass of water required for the CLSMs. The preparation process involved blending water, cement, and PCE for 120 seconds in a mortar mixer to create a binder milk. This step ensured an even distribution of cement particles. Subsequently, the red-bed mudstone was added and mixed for an additional 180 seconds, ensuring the uniformity of the mixes. This procedure resulted in the preparation of fresh CLSM mixes, as depicted in Fig. 3(a).

2.3.2 Packing density, void ratio, and WFT measurement

Packing density was measured using a wet packing method developed by Kwan et al. [26,27].

This method is based on the principle that the solid concentration varies with W/S. There exists an optimal W/S where the maximum solid concentration is achieved, indicating the water content is exactly sufficient to fill the voids and blend with the solid particles to form a paste. This maximum concentration, occurring when the particles are tightly packed against each other, is considered the packing density of the granular material. During the experiment, the W/S was systematically reduced, and the fresh CLSM was poured into an 80 mm × 80 mm cylindrical mold. The mix was then compacted by vibration and levelled with a straight edge, as shown in Fig. 3(b). Subsequently, the total mass of the mold and CLSM was measured using a balance. The packing density was calculated using Eqs. 1 and 2.

$$\varphi = \tau_{\max} \tag{1}$$

$$\tau = \frac{M / V}{u_w \rho_w + R_c \rho_c + + R_s \rho_s} \tag{2}$$

where φ is the packing density; τ is the solid concentration; V is the volume of the mold; M is the mass of CLSM in the mold; ρ_w is the density of water; ρ_c and ρ_s are the solid densities of cement and soil, respectively; u_w is the ratio of the volume of water to the solid particles volume; R_c and R_s are the volumetric ratios of cement and soil to the total solid volume, respectively. When the water content is larger than the water needed to fill up the voids of CLSMs, the excess water wraps on the surface of the solid particle to form a water film. After obtaining the wet packing density φ and solid concentration τ, the void ratio u_v, the minimum void ratio $u_{v,min}$, the excess water ratio u_e and WFT can be calculated using Eqs. 3 to 7.

$$u_v = \frac{1-\tau}{\tau} \tag{3}$$

$$u_{v,\min} = \frac{1-\varphi}{\varphi} \tag{4}$$

$$A = A_c R_c + A_s R_s \tag{5}$$

$$u_e = u_w - u_{v,\min} \tag{6}$$

$$WFT = \frac{u_e}{A} \tag{7}$$

where u_v is void ratio (defined as the ratio of the volume of void to the solid volume of the particles); $u_{v,min}$ is the minimum void ratio; A is the total specific surface area of cement and red-bed mudstone; A_c and A_s are the specific surface areas of cement and soil, respectively. WFT is calculated using a formula that assumes an average particle size, implying that each particle in CLSMs is coated with a water film of uniform thickness. Namely, WFT represents the average thickness of these water films surrounding the solid particles [34].

Given that WFT relates to particle spacing (λ) [35], λ in CLSMs can be calculated using Eq. (8).

$$\lambda = 2 \times WFT \tag{8}$$

2.3.3 Flowability test

Due to CLSM's exceptional flowability, which leads to minimal accumulation height, the conventional concrete slump test method is impractical. Thus, the flowability test adhered to the JHS A 313-1992 protocol, using an open-ended hollow acrylic cylinder with a height and diameter of 80 mm. The cylinder, placed on a glass plate, was filled with the fresh CLSM. It was then gradually lifted over 5 s, allowing the mix to disperse across the plate. The flow ceased, and the flow spread diameter was measured in two perpendicular directions. The average of these measurements indicated the CLSM's flowability, as shown in Fig. 3(c). To meet the flowability requirements specified in the

technical code (JHS A 313-1992), which mandates self-levelling to be no less than (180 ± 20) mm, this research sets the minimum self-levelling flowability at 160 mm.

2.3.4 Bleeding rate test

The bleeding rate was measured following ASTM C940-16. A 1000 mL graduated cylinder, filled with 800 mL of fresh CLSM, was covered with plastic parafilm to prevent evaporation, as depicted in Fig. 3(d). Record the readings of the upper surfaces of the CLSM mixture and the accumulated bleeding water at 15-minute intervals for the first hour. After the initial hour, continue recording at hourly intervals until two consecutive readings indicate no further bleeding. Bleeding rate was expressed as a percentage of the final bleeding water volume over the initial CLSM volume.

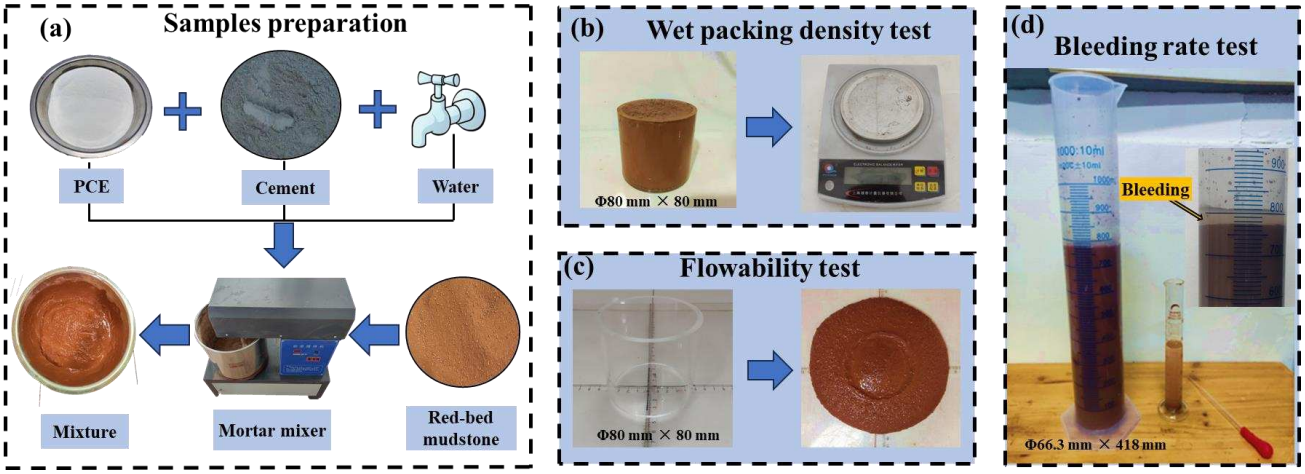

Figure 3. Laboratory test procedures

3 Results and analysis

In this section, the experimental outcomes are analyzed, exploring the dynamics between void ratio, solid concentration, packing density, WFT, flowability, and bleeding rate in relation to differing PCE dosages and W/S. This aims to study the impact of these variables on the properties of CLSMs, offering insights into their interdependencies and influence on CLSM's performance.

3.1 Experimental results

3.1.1 Void ratio and solid concentration

Fig. 4 displays the relationship between void ratio (u_v) and W/S by volume (u_w) for the CLSM. Initially, u_v decreases and then gradually increases with rising u_w. The minimum void ratio ($u_{v,min}$) is identified at the inflection point of this change, and the corresponding water content is defined as the basic water ratio [26]. When water is not added to the solid particles, the inter-particle friction makes it loosely pack, causing a high void ratio. Upon contact with water, particles are initially wetted, reducing inter-particle friction. The addition of water also leads to the formation of liquid bridges which, by increasing forces such as substrate suction and surface tension at the gas-liquid interface, reduce the particle spacing and thus lower u_v [36]. In line with the mechanics of unsaturated soils, as u_w increases, substrate suction and surface tension gradually reduce, slowing the decrease in u_v. When the CLSM approaches saturation, the effect of inter-particle friction can be negligible, making u_v the reaches a minimum. When u_w exceeds the basic water ratio, u_v begins to rise again, attributed to excess water forming a film around the particles, acting as a separation medium and increasing particle spacing. Note that when u_w is greater than the basic water ratio, theoretically u_w and u_v should be equal [26]. However, the tests show that u_v is lower than u_w. This is mainly due to the fact that the bleeding makes the u_w of CLSM mixture in the mold smaller than the mix design value, leading to the calculated u_v being lower than the actual value according to Eqs. 2 to 3.

The liquid limit of red-bed mudstone is 31.5%, closely aligned with the basic water ratio of the CLSM without PCE. Assuming the liquid limit of CLSM's particles is equivalent to the critical W/S, below this threshold, the water primarily forms a bound water film around the particles. Above this, to

quantify the impact of excess water and total specific surface areas on CLSM properties, excess water can be considered as a free water film of equal volume on the particles' surface. Additionally, Fig. 4 shows how u_v varies with u_w under different PCE dosages. Compared to the control group, PCE reduces both the basic water ratio and $u_{v,min}$, thereby lessening the amount of water needed to fill the voids, with greater PCE dosages amplifying this effect.

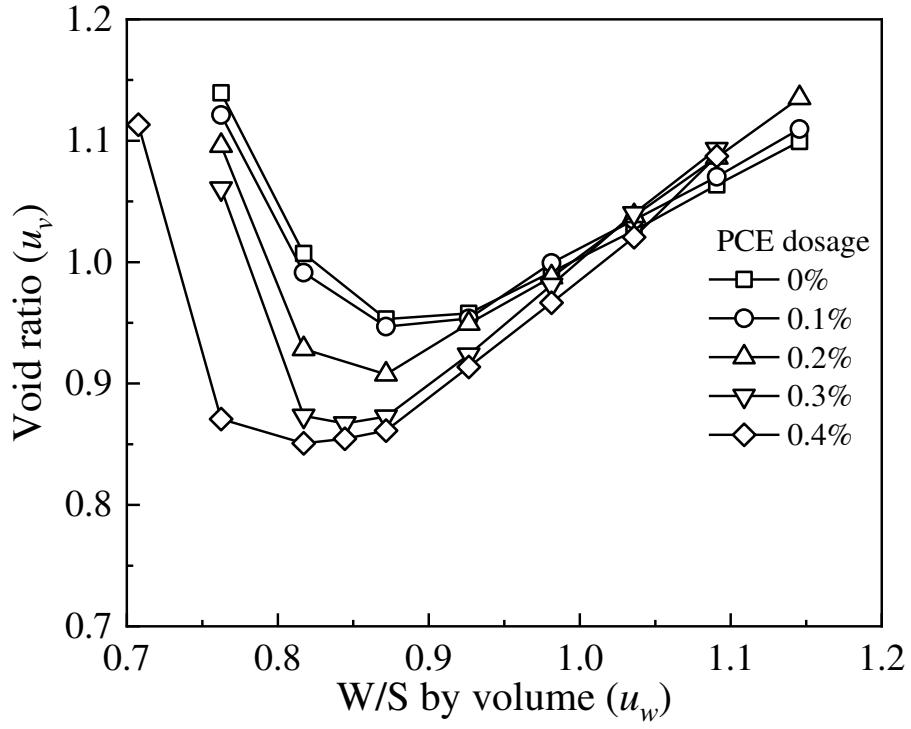

Figure 4. Variations of void ratio (u_v) with the W/S by volume (u_w) and PCE dosage

Fig. 5 demonstrates the variation of solid concentration (τ) in relation to the W/S by volume (u_w) and PCE dosage. It is observed that τ initially increases and then decreases as u_w rises, reaching a maximum τ for each mix. This maximum solid concentration represents the packing density [29]. The denser the packing, the more compactly the particles are arranged, resulting in a reduced need for water to fill the voids. Hence, for a given u_w, a higher packing density leads to more excess water to create a water film, enhancing the CLSM's flowability. Therefore, enhancing CLSM's packing density is a

feasible method to decrease the mixing water needed to achieve a desired flowability, thus facilitating easier flow in the mixes. The variations of τ with u_w and those of u_v with u_w exhibit opposite trends, yet their underlying causes and mechanisms are identical. The formation of liquid bridges decrease particle spacing, increasing the volume of solid particles per unit volume. When u_w exceeds the basic water ratio, the excess water acts as a separation medium, causing a decrease in the volume of the solid particles per unit volume. Section 3.1.2 further discusses the variation of maximum solid concentration with PCE dosage.

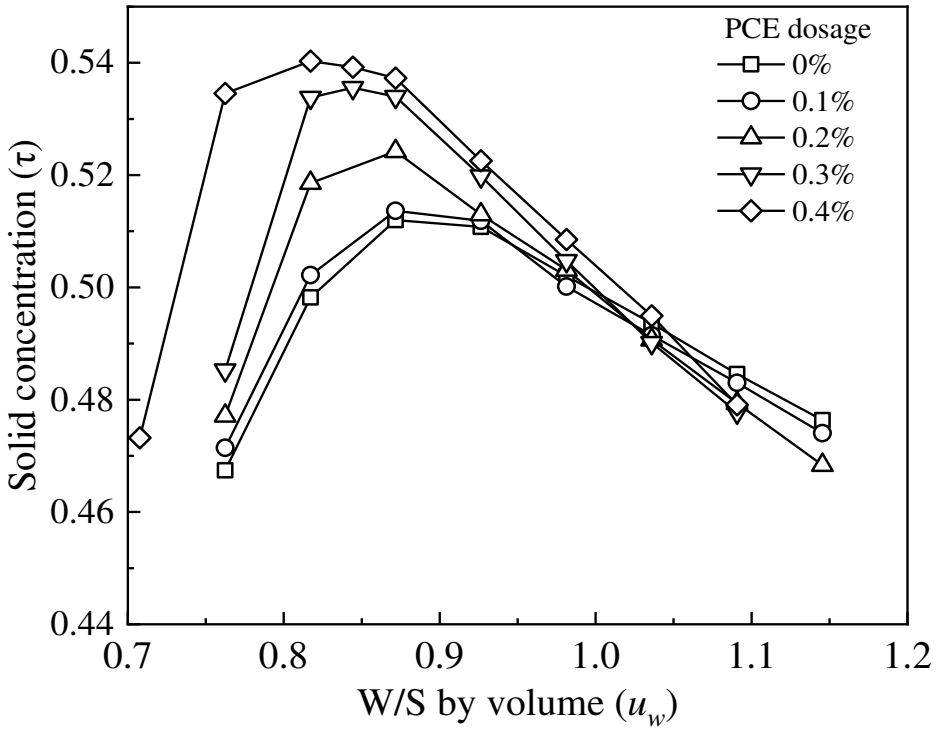

Figure 5. Variations of solid concentration (τ) with the W/S by volume (u_w) and PCE dosage

3.1.2 Packing density, minimum void ratio, and WFT

The results for packing density and minimum void ratio, in relation to increased PCE dosage, are depicted in Fig. 6. It was observed that, with increasing PCE dosage, the packing density of fresh CLSMs rose while the minimum void ratio decreased. This phenomenon aligns with findings in other

powder materials, such as cement paste, ultrafine-tailings cemented paste, and phosphorus gypsum paste [30–32]. In fresh soil-based CLSMs, cement and soil particles are susceptible to flocculation and agglomeration by intergranular van der Waals forces and electrostatic attraction [37]. This process traps a considerable amount of water, reducing workability. The introduction of PCE changes this dynamic. PCE molecules adsorb onto the surface of cement and soil particles, dispersing the agglomerates and filling gaps through electrostatic repulsion and steric hindrance, thereby densifying the CLSM particle packing [38]. Notably, a 0.4% PCE dosage significantly enhances this effect, increasing packing density by 5.33% and decreasing the minimum void ratio by 10.74% compared to the control group. In contrast, a 0.1% PCE dosage shows limited impact on soil-based CLSM, with only a 0.33% increase in packing density and a 0.67% decrease in minimum void ratio.

Previous studies [31] have identified a saturation point in polycarboxylate-based dosages in ultrafine-tailings cemented paste, beyond which further increases in PCE dosage yield minimal gains in packing density. In the current experiments, though a definitive saturated PCE dosage was not ascertained due to the gradient settings, a diminishing return in packing density increment was noted at a 0.4% PCE dosage compared to 0.2% and 0.3%. This variation and trend in minimum void ratio and packing density with PCE dosage not only quantified the impact of PCE on the dispersion of agglomerated particles but also helped in determining the saturated PCE dosage. Consequently, this provides a reference for appropriate PCE dosage level for soil-based CLSM. Considering both the effects of PCE and economic factors, a PCE dosage of 0.3% was recommended in this study.

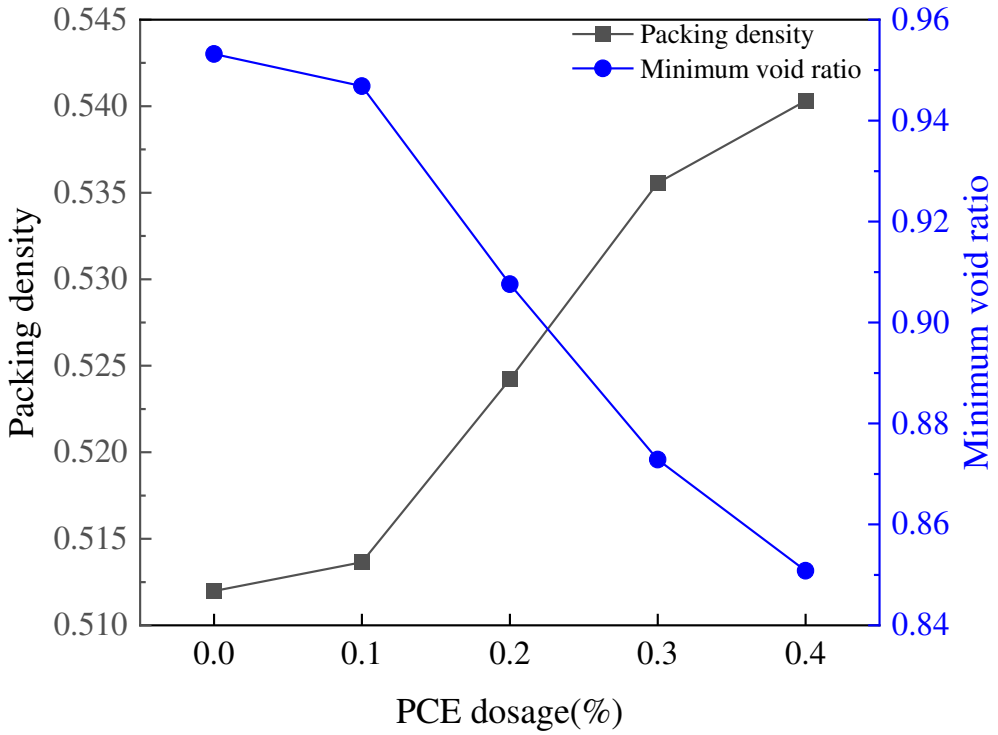

Figure 6. Variations of packing density and minimum void ratio with PCE dosage

Fig. 7 plots WFT against W/S and PCE dosage. WFT arises from a combination of the W/S, packing density, and the specific surface area of particles [28]. In the wet packing method, this specific surface area is considered constant [31]. A positive WFT value indicates the average thickness of water coating solid particles, whereas a negative value suggests insufficient water to fill the voids. For a constant mixing water content, an increase in WFT is noted as PCE dosage rises from 0% to 0.4%. This increase is attributed to a decrease in minimum void ratio, effectively reducing the water quantity needed to fill voids and, in turn, increase the excess water ratio. This results in a rise in WFT as per Eq. (7). Conversely, for a consistent PCE dosage, an increase in the W/S directly elevates the excess water ratio, consequently increasing the WFT in accordance with Eq. (7). Hence, the trend in the variation of excess water aligns with that of WFT for identical PCE dosages.

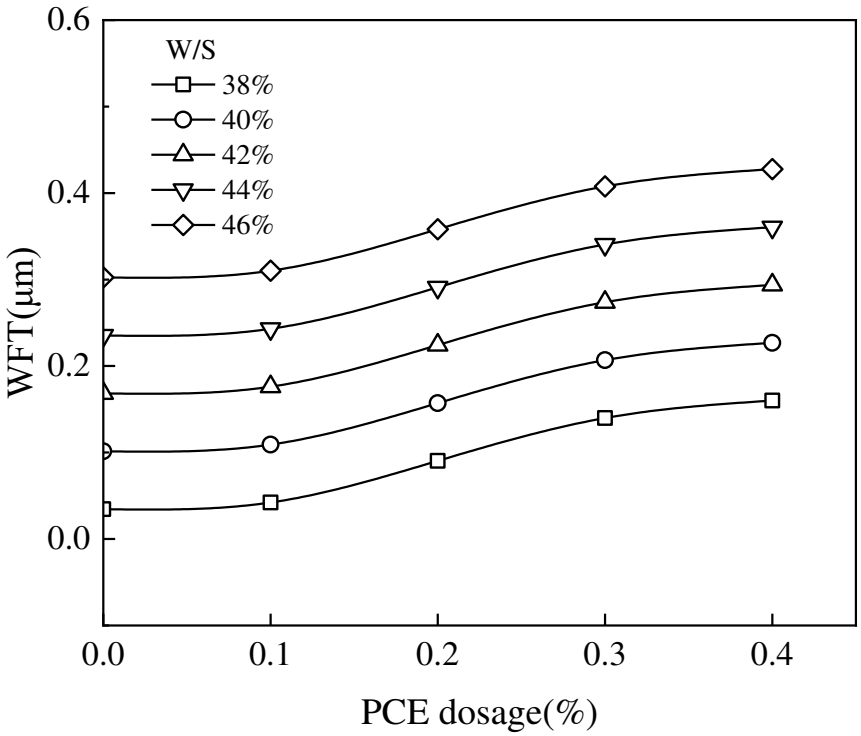

Figure 7. Variations of the WFT with the W/S and PCE dosage

3.1.3 Flowability

Fig. 8 illustrates the relationship between flowability, W/S, and PCE dosage. It is noted that when the W/S is below 44%, flowability does not meet the minimum self-levelling flowability of 160 mm without PCE addition. Within a certain range, flowability increases linearly with the W/S. This improvement is attributed to the more mixing water, which increases the WFT. Consequently, particle spacing widens, and the increased WFT acts as a lubricant, reducing friction and cohesiveness between particles and thus enhancing flowability [39].

Fig. 8 also reveals that the impact of PCE dosage on the flowability of fresh CLSMs significantly depends on the W/S. When the W/S ratio is as low as 32%, near the liquid limit of red-bed mudstone, the flowability increases from 81.5 mm to 121 mm with a PCE dosage increase from 0 to 0.4%, reflecting a 48.47% improvement. Conversely, at a W/S ratio of 40%, flowability increases from 111

mm to 344 mm with the same PCE dosage increase, showing an improvement over four times greater than at a W/S of 32%. Additionally, at a fixed W/S ratio of 32%, the flowability does not significantly increase compared to the control group, regardless of the PCE dosage. This is due to the fact that at a W/S ratio of 32%, the mixing water is just sufficient to fill the voids, resulting in a small WFT and significant colloidal attraction forces among particles, which hinder particle movement [40].

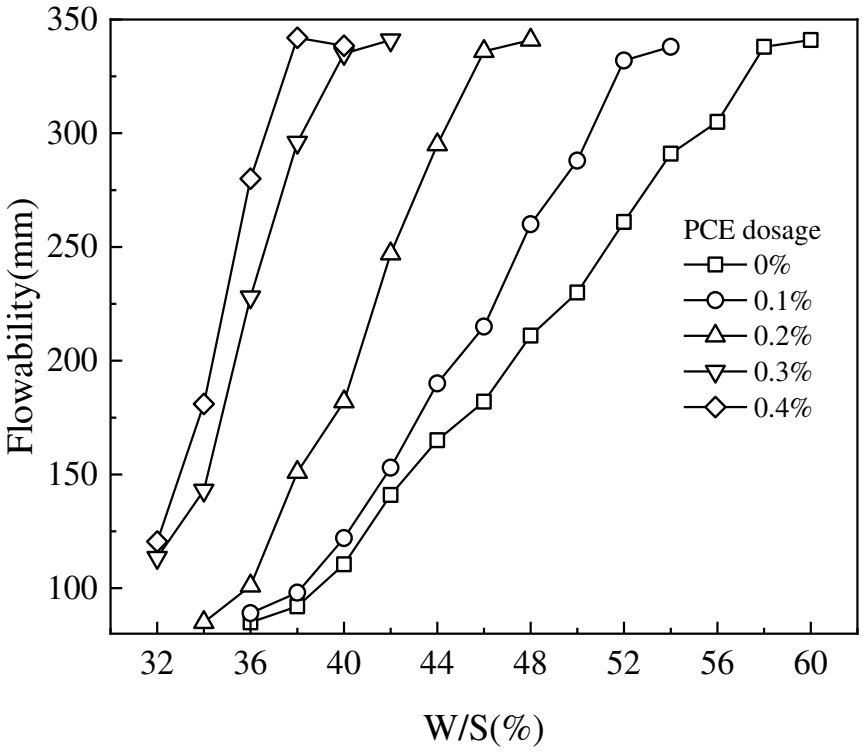

Figure 8. Variations of the flowability with the W/S and PCE dosage

3.1.4 Bleeding rate

Fig. 9 displays the relationship between the bleeding rate, W/S, and PCE dosage. The results indicate an increase in the bleeding rate with a rising W/S. This increase is primarily due to the fact that a higher W/S leads to an increased WFT, which expands particle spacing and subsequently reduces the cohesiveness of CLSMs.

Additionally, when comparing curves at different PCE dosages, it becomes apparent that the W/S

at which the bleeding rate starts increasing from zero is influenced by the PCE dosage. At a constant W/S, a higher PCE dosage in a CLSM correlates with a larger bleeding rate. For instance, at a fixed W/S of 42%, varying the PCE dosage from 0% to 0.4% significantly affects the bleeding rate, with fluctuations between 0% and 5.26%. Thus, adding PCE results in CLSMs starting to bleed at lower W/S. The combined effects of WFT and PCE dosage on this phenomenon are further discussed later in this paper.

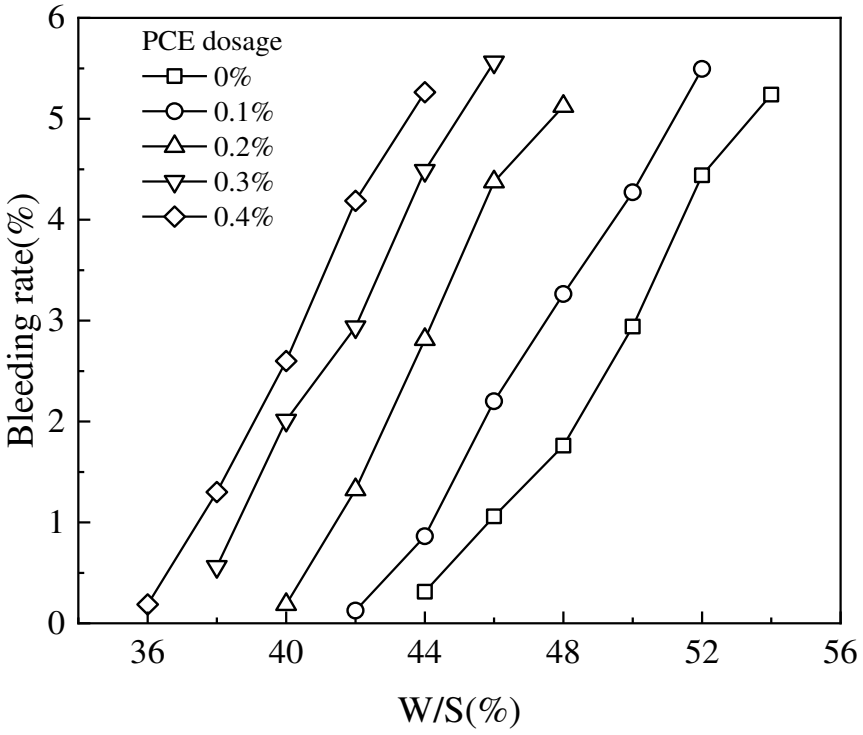

Figure 9. Variations of the bleeding rate with the W/S and PCE dosage

3.2 WFT effects and threshold analysis

3.2.1 Correlation between flowability and WFT

Fig. 10 illustrates the WFT and W/S of CLSMs required to achieve a standard flowability of 180 mm at varying PCE dosages. A comparison of the W/S in fresh CLSMs for standard flowability show a decrease in both W/S and WFT with increasing PCE. This decrease aids in clustering and bridging

hydration products and in densifying the microstructure [35], contributing to strength development of CLSM and addressing the contradiction between flowability and compressive strength in soil-based CLSM [21].

At a 0.3% PCE dosage, the fresh CLSM attains standard flowability with a WFT of 0.0924 μm, which is a 0.2418 μm and 72.4% reduction compared to the control group. However, further increases in PCE dosage do not significantly reduce the WFT needed for standard flowability [32]. For instance, at a 0.4% PCE dosage, the mix reaches standard flowability with a WFT of 0.0754 μm, marking a 0.2588 μm and 77.4% reduction compared to the control. This trend is attributed to PCE molecules on particle surfaces gradually reaching saturation, with additional increases in PCE dosage having a limited effect on enhancing repulsive forces between particles.

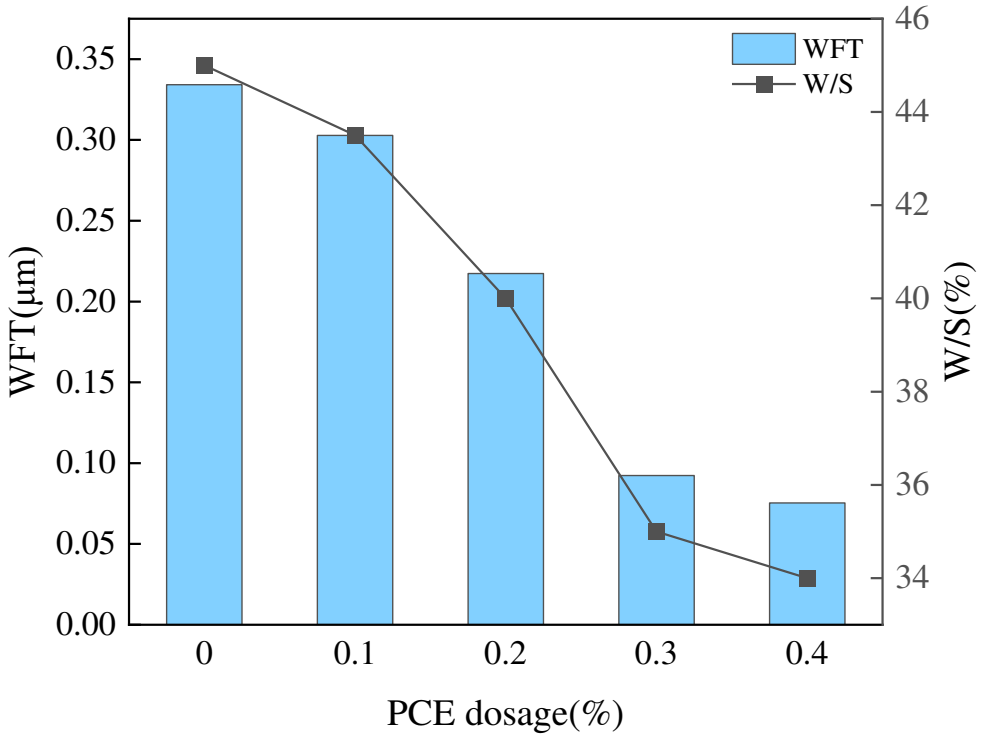

Figure 10. WFT and W/S at different PCE dosages for standard flowability

To examine the combined influence of WFT and PCE dosage on flowability, regression analysis

was conducted to derive fitting curves for varying PCE dosages, as shown in Fig. 11. The analysis yielded an R^2 value of 0.943, indicating flowability in CLSM is influenced by both PCE dosage and WFT. This analysis points to a strong linear positive correlation between flowability and WFT. The changing gradient of the fitting curves suggests that beyond a 0.3% PCE dosage, further increases in dosage do not significantly enhance flowability, also implying a maximum adsorption capacity of PCE on particle surfaces.

Within the 0 % to 0.4% range of PCE dosage, the flowability of fresh CLSMs increases more rapidly at higher PCE dosages. According to the regression equation, at 0%, 0.1%, 0.2%, 0.3% and 0.4% PCE dosage, the WFT becomes 0.1 μm thicker and the flowability increases by 31.4 mm, 39.3 mm, 57.6 mm, 98.2 mm and 117.7 mm, respectively. This suggests that while increasing PCE dosage can enhance packing density and consequently WFT, thereby improving flowability, PCE also directly influences flowability [30]. This effect is primarily due to the fact that higher PCE dosages enhance the repulsive impact of electrostatic force and steric hindrance on particle dispersion, facilitating CLSM movement by overcoming colloidal attraction [40]. However, for a given WFT, while an increase in PCE dosage markedly improves flowability, this effect diminishes with decreasing WFT. It's important to note that WFT is inversely non-linearly correlated with mix cohesiveness. Consequently, at low WFT levels, the dispersion effects of electrostatic force and steric hindrance struggle to overcome significant cohesiveness, resulting in a reduction in improvement effect of flowability.

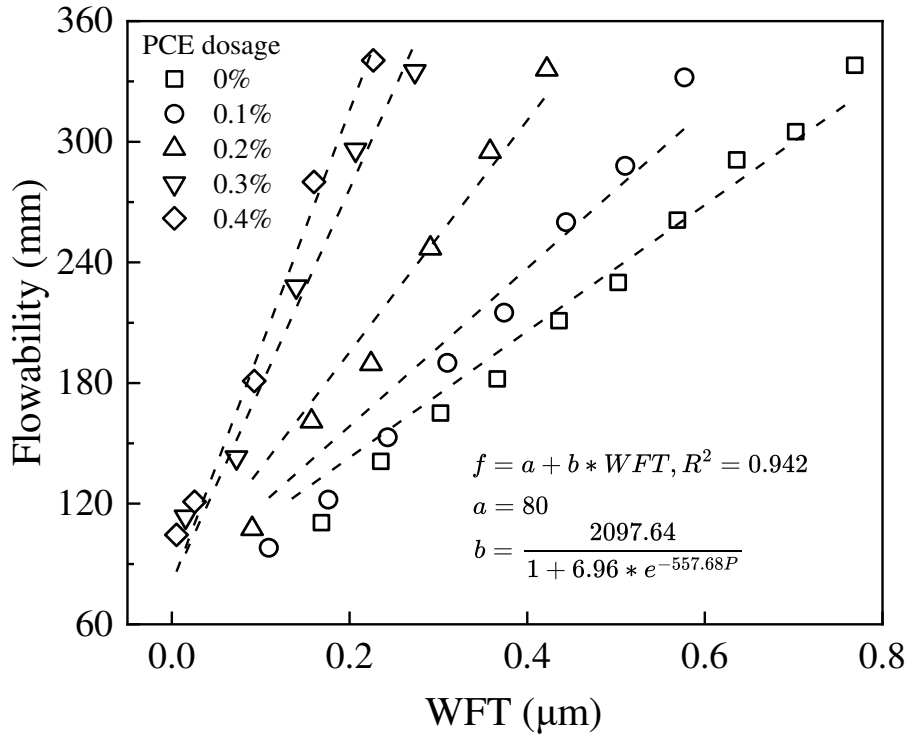

Figure 11. Combined effects of WFT and PCE dosage (*p*) on flowability (*f*)

3.2.2 Relationship between bleeding rate and WFT

Fig. 12 illustrates the relationship between the bleeding rate, WFT, and PCE dosage. It's observed that the bleeding rate generally rises with an increase in WFT, regardless of PCE dosage. To analyse the combined impact of WFT and PCE dosage, regression analysis was performed. This analysis yielded an R^2 value of 0.981, underscoring the significance of both WFT and PCE dosage in influencing the bleeding rate of fresh CLSMs. The bleeding rate not only increases linearly with rising WFT but also accelerates at higher PCE dosages. For instance, at the same WFT, a greater PCE dosage leads to a higher bleeding rate.

The influence of PCE dosage on the bleeding rate stems from two factors. Firstly, as PCE dosage increases, packing density also rises, which indirectly raises the excess water ratio and WFT, consequently reducing friction between particles and enhancing bleeding. Secondly, with an increase

in PCE, the colloidal attraction between particles diminishes due to the enhanced repulsive effects of electrostatic force and steric hindrance, thereby facilitating easier particle deposition under gravity.

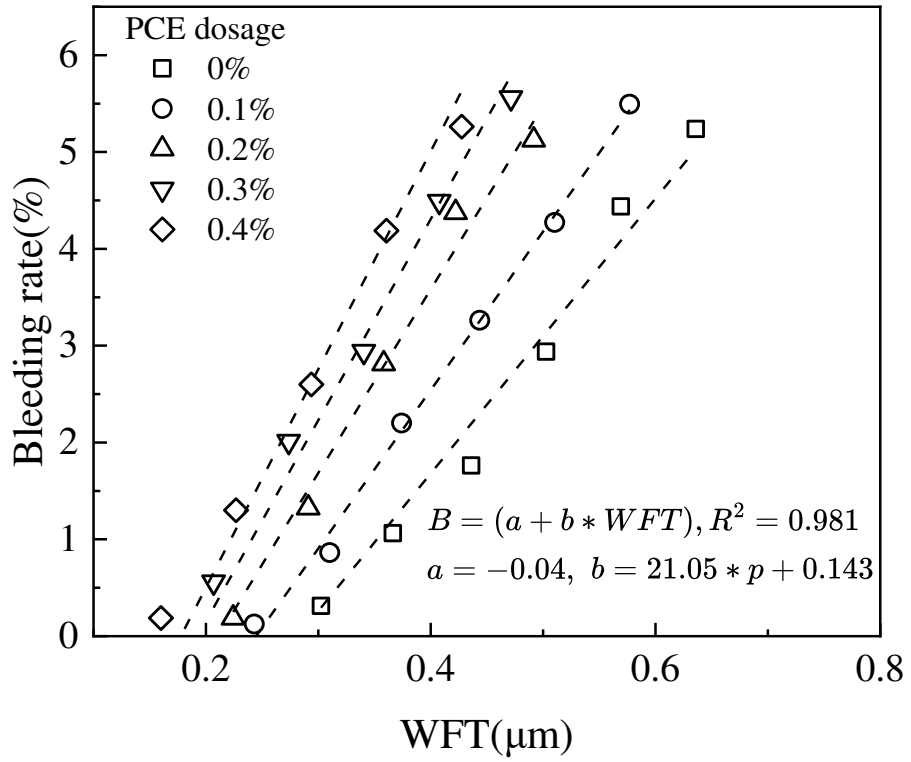

Figure 12. Combined effects of WFT and PCE dosage (p) on bleeding rate (B)

3.2.3 Thresholds of WFT

Figure 8 illustrates that each CLSM mixture achieves a peak flowability irrespective of the PCE dosage. Additionally, W/S at which maximum flowability occurs varies with the PCE dosage. Fig. 13 displays the WFT thresholds at maximum flowability for varying PCE dosages. WFT thresholds at maximum flowability, marks the critical point where WFT no longer affects CLSM flowability. It is evident that the WFT required to reach maximum flowability depends on the PCE dosage. In other words, the WFT thresholds at maximum flowability differ across PCE dosages and it decreases exponentially as PCE dosage increases.

Flowability in cement paste is primarily governed by colloidal interactions, gravity, and Brownian

force [41]. In a steady state, Brownian motion is negligible compared to the attractive colloidal interactions between cement grains [42]. Without PCE, Van der Waals forces dominate other colloidal interactions and are inversely proportional to particle spacing (λ) [39,43]. However, with PCE addition, colloidal interactions also include the repulsive effects of electrostatic force and steric hindrance. Therefore, at lower WFT levels, colloidal attraction is stronger, and the repulsive effect provided by PCE only marginally reduces this attraction. This explains why improvements in CLSM flowability are not significant at low WFT levels, regardless of PCE dosage. When WFT exceeds a threshold, changes in WFT have a smaller impact on colloidal attraction [44], making flowability less sensitive to WFT changes. Kwan et al. [30] noted that the addition of a superplasticizer has two major effects: (1) reducing agglomeration, thus increasing packing density and WFT, and (2) reducing cohesiveness, making the mortar more flowable. Specifically, an increase in WFT reduces colloidal attraction between particles, while the repulsive forces from PCE also diminish colloidal attraction. Both effects facilitate easier particle flow. At higher PCE dosages, the repulsive forces are stronger, leading to a reduction in the WFT thresholds at maximum flowability.

The bleeding rate is a common measure of subsidence in CLSMs, with stability considered at rates below 5% [45,46]. Perrot et al. [41] assert that stable suspension conditions arise from a balance between colloidal interactions and gravity. Fig. 13 also indicates that the WFT thresholds at a 5% bleeding rate decrease with increasing PCE dosage. This is because PCE addition reduces colloidal attraction, making particles more susceptible to gravitational deposition. Furthermore, comparison of the two curves shows that PCE presence can deliver higher flowability while maintaining acceptable bleeding rate.

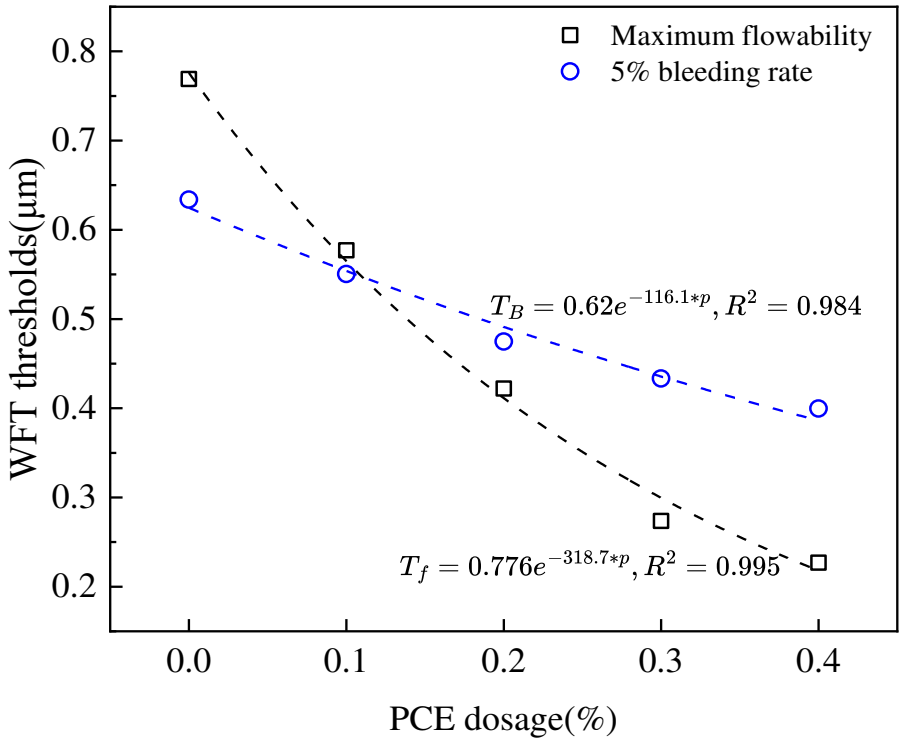

Figure 13. Variations of WFT thresholds with PCE dosage (p) for maximum flowability and 5% bleeding rate (B): T_f, WFT threshold for maximum flowability; T_B, WFT threshold for 5% bleeding rate

3.3 PCE mechanisms and long-term CLSM performance analysis

This study aims to enhance flowability at a low W/S in soil-based CLSM by incorporating PCE, addressing the existing conflict between flowability and compressive strength. However, soil-based CLSM with PCE is under-researched, and the mechanisms of PCE's influence require further exploration. Fig. 14 illustrates these mechanisms, primarily based on experimental results and colloidal interactions. It is widely accepted that PCE's anionic groups anchor onto particle surfaces, creating electrostatic repulsion, while its side chains, extending into the solution, provide steric hindrance when particle spacing is small. This steric hindrance is considered the primary factor in PCE's dispersion effects [36].

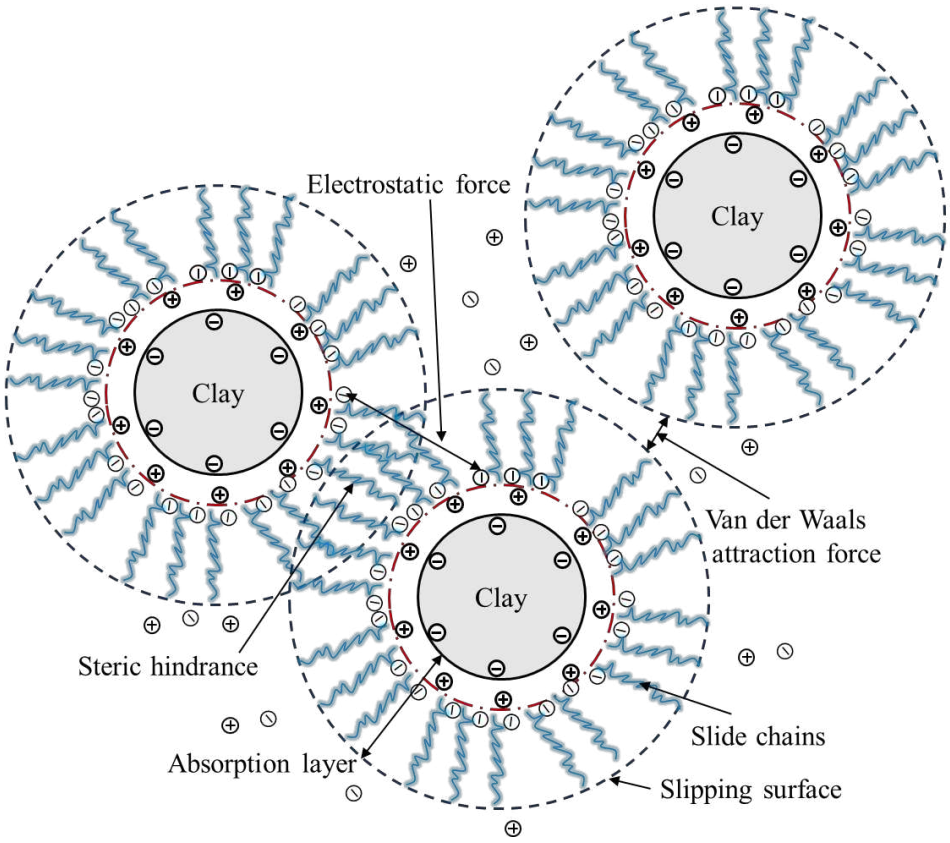

Figure 14. Conceptual illustration of adsorption and repulsion between soil particles and PCE [21]

All samples were prepared and their flowability tested within a short timeframe, excluding cement hydration considerations. However, for CLSM applications unsuitable for on-site mixing and requiring long transport times, the impact of cement hydration is significant. Moreover, the wet packing method assumes complete particle dispersion, treating the specific surface area of the particle system as constant [30,31]. While PCE addition disperses agglomerated particles and increases packing density, the consequent alterations in particle surface area and water release have not been accounted for. Therefore, understanding how CLSM flowability changes over time with PCE addition and quantitatively analysing water release and particle agglomeration in response to different PCE dosages is important in the future.

4 Conclusions

In this study, a wet packing method was employed to determine the packing density of fresh CLSMs. WFT was then calculated based on test results, W/S, and the specific surface area of particles. A range of fresh CLSM mixes with varying PCE dosages and W/S were prepared to assess packing density, WFT, flowability, and bleeding rate. Additionally, WFT theory was used to analyse the combined impacts of PCE dosage and WFT on the flowability and bleeding rate. The experimental findings led to the following conclusions:

a) The packing density of CLSM shows a non-linear enhancement with increasing PCE dosage. Specifically, within the PCE dosage range of 0.1% to 0.3%, there is a marked increase in packing density, while increments in packing density are less pronounced when the PCE dosage is below 0.1% or exceeds 0.3%. At a PCE dosage of 0.4%, the packing density improves by 5.53% compared to the control group.

b) The addition of PCE significantly enhances flowability, allowing fresh CLSMs to achieve standard flowability at lower W/S or WFT. This resolves the existing conflict between flowability and compressive strength in soil-based CLSM. Flowability improvement is influenced by both WFT and PCE dosage. Considering the effects of PCE, a PCE dosage of 0.3% is recommended for the material in this study.

c) Regression analysis exploring the combined effects of PCE dosage and WFT on flowability and bleeding rate yielded R2 values of 0.943 and 0.981, respectively. The flowability and bleeding rate increase linearly with rising WFT, with more pronounced enhancements at higher PCE dosages. Additionally, at a constant WFT, the impact of PCE dosage on flowability and bleeding rate

diminishes with decreasing WFT.

d) The addition of PCE not only increases WFT but also provides repulsive forces (electrostatic force and steric hindrance), reducing colloidal attraction and thus facilitating particle movement or deposition under gravity. The WFT thresholds at maximum flowability and a 5% bleeding rate decrease with increasing PCE dosage due to reduced colloidal attraction. The practical significance of these thresholds is that they indicate the critical point where WFT no longer affects flowability and represent the limit for WFT to meet bleeding rate requirements, respectively, which can provide a reference for the design of mixing proportion for soil-based CLSM.

Acknowledgements

This research was funded by the National Natural Science Foundation of China (Grant No. 52078435), the Natural Science Foundation of Sichuan Province (Grant No. 2023NSFSC0391), the Overseas Expertise Introduction Project for Discipline Innovation ("111 Project ", Grant No. B21011), Science Foundation of China Academy of Railway Sciences Corporation Limited (No. 2022YJ098), and the Royal Society UK (IEC\NSFC\211306).

References

[1] M. Haas, L. Mongeard, L. Ulrici, L. D'Aloïa, A. Cherrey, R. Galler, M. Benedikt, Applicability of excavated rock material: A European technical review implying opportunities for future tunnelling projects, J. Clean. Prod. 315 (2021) 128049. https://doi.org/10.1016/j.jclepro.2021.128049.

[2] K. Kataguiri, M.E.G. Boscov, C.E. Teixeira, S.C. Angulo, Characterization flowchart for assessing the potential reuse of excavation soils in Sao Paulo city, J. Clean. Prod. 240 (2019) 118215. https://doi.org/10.1016/j.jclepro.2019.118215.

[3] N. Zhang, H. Zhang, G. Schiller, H. Feng, X. Gao, E. Li, X. Li, Unraveling the global warming mitigation potential from recycling subway-related excavated soil and rock in China via life cycle assessment, Integrated Environmental Assessment and Management. 17 (2021) 639–650.

https://doi.org/10.1002/ieam.4376.
[4] M. Arm, O. Wik, C.J. Engelsen, M. Erlandsson, O. Hjelmar, M. Wahlström, How does the European recovery target for construction & demolition waste affect resource management?, Waste Biomass Valor. 8 (2017) 1491–1504. https://doi.org/10.1007/s12649-016-9661-7.
[5] H. Duan, T.R. Miller, G. Liu, V.W.Y. Tam, Construction debris becomes growing concern of growing cities, Waste Manag. 83 (2019) 1–5. https://doi.org/10.1016/j.wasman.2018.10.044.
[6] N. Zhang, H. Duan, P. Sun, J. Li, J. Zuo, R. Mao, G. Liu, Y. Niu, Characterizing the generation and environmental impacts of subway-related excavated soil and rock in China, J. Clean. Prod. 248 (2020) 119242. https://doi.org/10.1016/j.jclepro.2019.119242.
[7] I. Bozbey, E. Guler, Laboratory and field testing for utilization of an excavated soil as landfill liner material, Waste Manage. (Oxford) 26 (2006) 1277–1286. https://doi.org/10.1016/j.wasman.2005.10.014.
[8] G. Feng, Q. Luo, T. Wang, D.P. Connolly, K. Liu, Frequency spectra analysis of vertical stress in ballasted track foundations: influence of train configuration and subgrade depth, Transp. Geotech. 44 (2024) 101167. https://doi.org/10.1016/j.trgeo.2023.101167.
[9] H. Liu, Q. Luo, M.H. El Naggar, L. Zhang, T. Wang, Centrifuge modeling of stability of embankment on soft soil improved by rigid columns, J. Geotech. Geoenviron. Eng. 149 (2023) 04023069. https://doi.org/10.1061/JGGEFK.GTENG-11314.
[10] ACI 229R-13: Report on controlled low-strength materials, ACI Committee 229, American Concrete Institute (ACI), Farmington Hills, MI, 2013.
[11] Y. Kim, T.M. Do, H. Kim, G. Kang, Utilization of excavated soil in coal ash-based controlled low strength material (CLSM), Constr. Build. Mater. 124 (2016) 598–605. https://doi.org/10.1016/j.conbuildmat.2016.07.053.
[12] A.J. Finney, E.F. Shorey, J. Anderson, Use of native soil in place of aggregate in controlled low strength material (CLSM), in: Pipelines 2008, American Society of Civil Engineers, Atlanta, Georgia, United States, 2008: pp. 1–13. https://doi.org/10.1061/40994(321)124.
[13] C.A. Lowitz, G. DeGroot, Soil-cement pipe bedding: Canadian river aqueduct, J. Constr. Div. 94 (1968) 17–33. https://doi.org/10.1061/JCCEAZ.0000211.
[14] C.-F. Chang, J.-W. Chen, Development and production of ready-mixed soil Material, J. Mater. Civ. Eng. 18 (2006) 792–799. https://doi.org/10.1061/(ASCE)0899-1561(2006)18:6(792).
[15] S. Jian, C. Cheng, J. Wang, Y. Lv, B. Li, D. Wang, C. Wang, H. Tan, B. Ma, Effect of sulfonated acetone formaldehyde on the properties of high-fluid backfill materials, Constr. Build. Mater. 327 (2022) 126795. https://doi.org/10.1016/j.conbuildmat.2022.126795.
[16] Z. Huang, T. Tong, H. Liu, W. Qi, Properties of soil-based flowable fill under drying–wetting and freeze–thaw actions, Sustainability. 15 (2023) 2390. https://doi.org/10.3390/su15032390.
[17] J. Qian, Y. Hu, J. Zhang, W. Xiao, J. Ling, Evaluation the performance of controlled low strength material made of excess excavated soil, J. Clean. Prod. 214 (2019) 79–88. https://doi.org/10.1016/j.jclepro.2018.12.171.
[18] A.J. Puppala, B. Chittoori, A. Raavi, Flowability and density characteristics of controlled low-strength material using native high-plasticity clay, J. Mater. Civ. Eng. 27 (2015) 06014026. https://doi.org/10.1061/(ASCE)MT.1943-5533.0001127.
[19] L. Wang, W. Feng, S.A.M. Lazaro, X. Li, Y. Cheng, Z. Wang, Engineering properties of soil-based controlled low-strength materials made from local red mud and silty soil, Constr. Build.

Mater. 358 (2022) 129453. https://doi.org/10.1016/j.conbuildmat.2022.129453.
[20] X. Wan, J. Ding, N. Jiao, S. Zhang, J. Wang, C. Guo, Preparing controlled low strength materials (CLSM) using excavated waste soils with polycarboxylate superplasticizer, Environ. Earth Sci. 82 (2023) 214. https://doi.org/10.1007/s12665-023-10884-5.
[21] S. Zhang, N. jiao, J. Ding, C. Guo, P. Gao, X. Wei, Utilization of waste marine dredged clay in preparing controlled low strength materials with polycarboxylate superplasticizer and ground granulated blast furnace slag, J. Build. Eng. (2023) 107351. https://doi.org/10.1016/j.jobe.2023.107351.
[22] A.K.H. Kwan, L.G. Li, Combined effects of water film thickness and paste film thickness on rheology of mortar, Mater. Struct. 45 (2012) 1359–1374. https://doi.org/10.1617/s11527-012-9837-y.
[23] Y. Ghasemi, M. Emborg, A. Cwirzen, Effect of water film thickness on the flow in conventional mortars and concrete, Mater. Struct. 52 (2019) 62. https://doi.org/10.1617/s11527-019-1362-9.
[24] L.G. Li, A.K.H. Kwan, Concrete mix design based on water film thickness and paste film thickness, Cem. Concr. Compos. 39 (2013) 33–42. https://doi.org/10.1016/j.cemconcomp.2013.03.021.
[25] C. Zhang, A. Wang, M. Tang, X. Liu, The filling role of pozzolanic material, Cem. Concr. Res. 26 (1996) 943–947. https://doi.org/10.1016/0008-8846(96)00064-6.
[26] H.H.C. Wong, A.K.H. Kwan, Packing density of cementitious materials: part 1—measurement using a wet packing method, Mater. Struct. 41 (2008) 689–701. https://doi.org/10.1617/s11527-007-9274-5.
[27] A.K.H. Kwan, H.H.C. Wong, Effects of packing density, excess water and solid surface area on flowability of cement paste, Adv. Cem. Res. 20 (2008) 1–11. https://doi.org/10.1680/adcr.2008.20.1.1.
[28] H.H.C. Wong, A.K.H. Kwan, Rheology of cement paste: role of excess water to solid surface area ratio, J. Mater. Civ. Eng. 20 (2008) 189–197. https://doi.org/10.1061/(ASCE)0899-1561(2008)20:2(189).
[29] W.W.S. Fung, A.K.H. Kwan, Role of water film thickness in rheology of CSF mortar, Cem. Concr. Compos. 32 (2010) 255–264. https://doi.org/10.1016/j.cemconcomp.2010.01.005.
[30] A.K.H. Kwan, W.W.S. Fung, Roles of water film thickness and SP dosage in rheology and cohesiveness of mortar, Cem. Concr. Compos. 34 (2012) 121–130. https://doi.org/10.1016/j.cemconcomp.2011.09.016.
[31] Z. Guo, J. Qiu, H. Jiang, J. Xing, X. Sun, Z. Ma, Flowability of ultrafine-tailings cemented paste backfill incorporating superplasticizer: Insight from water film thickness theory, Powder Techno. 381 (2021) 509–517. https://doi.org/10.1016/j.powtec.2020.12.035.
[32] L. Wu, Z. Tao, R. Huang, Y. Zhang, S. Liao, J. Ye, Roles of water film thickness and polycarboxylate dosage in the flow spread of phosphorus building gypsum, J. Build. Eng. 74 (2023) 106911. https://doi.org/10.1016/j.jobe.2023.106911.
[33] Y. Zhu, D. Liu, G. Fang, H. Wang, D. Cheng, Utilization of excavated loess and gravel soil in controlled low strength material: laboratory and field tests, Constr. Build. Mater. 360 (2022) 129604. https://doi.org/10.1016/j.conbuildmat.2022.129604.
[34] L.G. Li, A.K.H. Kwan, Effects of superplasticizer type on packing density, water film thickness

and flowability of cementitious paste, Constr. Build. Mater. 86 (2015) 113–119. https://doi.org/10.1016/j.conbuildmat.2015.03.104.
[35] Y. Guo, T. Zhang, J. Wei, Q. Yu, S. Ouyang, Evaluating the distance between particles in fresh cement paste based on the yield stress and particle size, Constr. Build. Mater. 142 (2017) 109–116. https://doi.org/10.1016/j.conbuildmat.2017.03.055.
[36] M. Zhao, X. Zhang, Y. Zhang, Effect of free water on the flowability of cement paste with chemical or mineral admixtures, Constr. Build. Mater. 111 (2016) 571–579. https://doi.org/10.1016/j.conbuildmat.2016.02.057.
[37] Q. Li, Y. Fan, Rheological evaluation of nano-metakaolin cement pastes based on the water film thickness, Constr. Build. Mater. 324 (2022) 126517. https://doi.org/10.1016/j.conbuildmat.2022.126517.
[38] X. Qin, Y. Cao, H. Guan, Q. Hu, Z. Liu, J. Xu, B. Hu, Z. Zhang, R. Luo, Resource utilization and development of phosphogypsum-based materials in civil engineering, J. Clean. Prod. 387 (2023) 135858. https://doi.org/10.1016/j.jclepro.2023.135858.
[39] H. Liu, X. Sun, H. Du, H. Lu, Y. Ma, W. Shen, Z. Tian, Effects and threshold of water film thickness on multi-mineral cement paste, Cem. Concr. Compos. 112 (2020) 103677. https://doi.org/10.1016/j.cemconcomp.2020.103677.
[40] H. Qi, B. Ma, H. Tan, Y. Su, Z. Jin, C. Li, X. Liu, Q. Yang, Z. Luo, Polycarboxylate superplasticizer modified by phosphate ester in side chain and its basic properties in gypsum plaster, Constr. Build. Mater. 271 (2021) 121566. https://doi.org/10.1016/j.conbuildmat.2020.121566.
[41] A. Perrot, T. Lecompte, H. Khelifi, C. Brumaud, J. Hot, N. Roussel, Yield stress and bleeding of fresh cement pastes, Cem. Concr. Res. 42 (2012) 937–944. https://doi.org/10.1016/j.cemconres.2012.03.015.
[42] N. Roussel, A. Lemaître, R.J. Flatt, P. Coussot, Steady state flow of cement suspensions: A micromechanical state of the art, Cem. Concr. Res. 40 (2010) 77–84. https://doi.org/10.1016/j.cemconres.2009.08.026.
[43] R.J. Flatt, Dispersion forces in cement suspensions, Cem. Concr. Res. 34 (2004) 399–408. https://doi.org/10.1016/j.cemconres.2003.08.019.
[44] H. Liu, X. Sun, Y. Wang, X. Lu, H. Du, Z. Tian, Study on the influence of silica fume (SF) on the rheology, fluidity, stability, time-varying characteristics, and mechanism of cement paste, Materials. 15 (2022) 90. https://doi.org/10.3390/ma15010090.
[45] M. Gabr, Controlled low-strength material using fly ash and AMD sludge, J. Hazard. Mater. 76 (2000) 251–263. https://doi.org/10.1016/S0304-3894(00)00202-8.
[46] D.Y.S. Yan, I.Y. Tang, I.M.C. Lo, Development of controlled low-strength material derived from beneficial reuse of bottom ash and sediment for green construction, Constr. Build. Mater. 64 (2014) 201–207. https://doi.org/10.1016/j.conbuildmat.2014.04.087.